Collider probe of heavy additional Higgs bosons solving the muon $g-2$ and dark matter problems

Monika Blanke[1,2,*] and Syuhei Iguro[1,2,†]
[1] *Institute for Theoretical Particle Physics (TTP), Karlsruhe Institute of Technology (KIT), Engesserstraße 7, 76131 Karlsruhe, Germany*
[2] *Institute for Astroparticle Physics (IAP), Karlsruhe Institute of Technology (KIT), Hermann-von-Helmholtz-Platz 1, 76344 Eggenstein-Leopoldshafen, Germany*

We study the Large Hadron Collider (LHC) search potential of a $\mathbb{Z}_4$-based two Higgs doublet model which can simultaneously explain the muon $g-2$ anomaly and the observed dark matter. The neutral scalars in the second Higgs doublet couple to μ and τ and largely contribute to the muon anomalous magnetic moment through the one-loop diagram involving τ and scalars. An additional singlet scalar which is charged under the discrete symmetry can be a dark matter candidate. An upper limit on the scalar mass originates from the unitarity constraint, and the $\mu\tau$ flavor violating nature of the scalars predicts non-standard signatures at the LHC. However, the previously proposed $\mu^\pm\mu^\pm\tau^\mp\tau^\mp$ signal via the electroweak heavy neutral scalar pair production at the LHC loses sensitivity for increasing scalar mass. We revisit this model and investigate the LHC prospects for the single production of the $\mu\tau$ flavor violating neutral scalar. It is shown that the single scalar process helps to extend the LHC reach for the 1 TeV mass regime of the scenario. The search potential at the high energy LHC is also discussed.

Keywords: Multi-Higgs Models, Muon $g-2$, Dark Matter, Large Hadron Collider

I. INTRODUCTION

Most experimental results so far support the standard model (SM) of particle physics. However, the SM falls short of explaining dark matter, the baryon asymmetry of the universe, neutrino masses and so on. Each of these problem has many possible solutions, and thus more experimental hints are required to specify the correct new physics (NP) scenario. One of the most notorious and long-lived discrepancies between the SM prediction and the measurement exists in the muon anomalous magnetic moment (a_μ) [1–3]. The comparison of the SM prediction and the experimental value is given as

$$\Delta a_\mu = a_\mu^{\rm exp} - a_\mu^{\rm SM} = (2.51 \pm 0.59) \times 10^{-9}. \qquad (1)$$

The SM prediction is taken from the white paper [1] which is mainly based on the data-driven determination of the hadronic vacuum-polarization contribution [4–7].[#1] It is known that the discrepancy is of the same order as the electroweak contribution, i. e. a new $\mathcal{O}(100)$ GeV weakly coupled particle can explain the discrepancy. However, no signal of NP at this scale has been found at the Large Hadron Collider (LHC) so far. This fact implies that in order to explain the discrepancy in terms of NP, some enhancement mechanism in the NP contribution to $g-2$ is necessary.[#2]

A popular method to enhance the $g-2$ contribution is the introduction of a new flavor-violating particle. The dipole operator underlying $g-2$ requires a chirality flip, which corresponds to the muon mass within flavor-conserving scenarios. A one-loop contribution involving a $\mu\tau$ flavor-violating particle is instead enhanced by a factor of $m_\tau/m_\mu \simeq 17$ [15–43].[#3] This mechanism can lift the mass scale of the new particle by more than a factor of four. However, lepton flavor-violating (LFV) interactions are stringently constrained and easily spoil the model if the particle also has lepton flavor-conserving couplings. Therefore one needs to ensure the absence of flavor-diagonal couplings for the τ mass enhanced muon $g-2$ solution to be viable.

This specific coupling alignment can be realized by a discrete $\mathbb{Z}_4$ flavor symmetry within the two Higgs doublet model (2HDM) [28]. In this model the $g-2$ contribution is proportional to the $\mu\tau$ LFV coupling and the mass difference of the additional neutral scalars. Recently it was proposed that the singlet scalar extension of the model can explain the relic density of the dark matter (DM) through the thermal freeze-out mechanism [43]. The $\mathbb{Z}_4$ symmetry is then used both to stabilize the DM candidate and also to realize the flavor alignment.

Since the new scalars are quark-phobic within the $\mathbb{Z}_4$-based model, their production cross section at the LHC is not large. However, the unique coupling structure predicts that the neutral scalars decay into $\mu^\pm\tau^\mp$. Previously we pointed out the smoking-gun signature of a $\mu^\pm\mu^\pm\tau^\mp\tau^\mp$ final state via electroweak scalar pair produc-

* monika.blanke@kit.edu
† igurosyuhei@gmail.com

#1 We note that the estimate based on the recent lattice simulation differs and is more consistent with the measured muon $g-2$ [8, 9]. Recent results from other lattice groups are converging towards the BMW result [8, 10]. However, the lattice results are in tension with the low energy $\sigma(e^+e^- \to \text{hadrons})$ data [11–13], so that further clarification is needed. In this paper we consider the discrepancy as quoted in Eq. (1).

#2 See Ref. [14] for a recent review.

#3 Due to the loop function, scalar mediators receive a further enhancement.

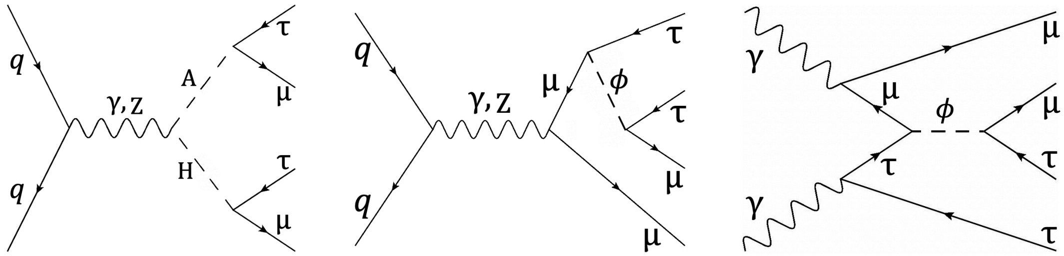

FIG. 1. Representative Feynman diagrams that contribute to the $\mu^{\pm}\mu^{\pm}\tau^{\mp}\tau^{\mp}$ signal at the LHC. The left corresponds to electroweak pair production channel. The middle and right diagrams correspond to the single production process where ϕ denotes A or H. In addition, there are also those obtained by exchanging μ and τ which are included in our numerical calculation.

tion (left of Fig. 1) with a special focus on the case where all Yukawa and scalar potential couplings are smaller than one [30]. We argued that the full Run 2 data set can test the model up to 500 GeV scalar mass thanks to the very unique double $\mu\tau$ LFV resonance nature of the signal events. However, if we accept relatively large coupling of $\mathcal{O}(1)$, the model can still explain the discrepancy with 1 TeV scalars.

In this paper we revisit the model's collider prospects in the presence of larger couplings. The pair production cross section is governed only by the electroweak coupling and decreases rapidly when the scalars get heavier. We thus propose the single scalar production process (middle and right of Fig. 1) to assist to cover the heavier scalar scenario. To search for the heavy lepto-philic bosons, it is known that the inclusion of photon-initiated processes is important [34]. We combine those processes and evaluate the search potential at the future LHC.

The layout of the paper is given as follows. In Sec. II, we briefly introduce our setup of the 2HDM and review the muon $g-2$ explanation. There we determine how heavy the scalar can be and discuss relevant constraints. In Sec. III, we focus on the collider phenomenology and show the impact of the single scalar production process to evaluate the future LHC reach. Sec. IV is devoted to the summary and discussion.

II. MODEL AND MUON $g-2$

We consider a two Higgs doublet model with an additional scalar singlet (S) and a discrete $\mathbb{Z}_4$ symmetry under which the Higgs and lepton fields transform as given in Tab. I. The gauge charge assignments of other SM fields, e. g. quarks, are the same as in the SM, and they trivially transform under $\mathbb{Z}_4$.#4

We assume the $\mathbb{Z}_4$ symmetry to be unaffected by electroweak symmetry breaking, so that the two Higgs doublets $H_{1,2}$ are in the Higgs basis [44, 45] in which only one Higgs doublet has a non-vanishing vacuum expectation value of $v \simeq 246$ GeV. In this basis, the two Higgs doublets can be decomposed as

Field	H_1	H_2	$(L_e,\, L_\mu,\, L_\tau)$	$(e_R,\, \mu_R,\, \tau_R)$	S
SM gauge	$(1,2)_{1/2}$	$(1,2)_{1/2}$	$(1,2)_{-1/2}$	$(1,1)_{-1}$	$(1,1)_0$
$\mathbb{Z}_4$	1	-1	$(1,\, i,\, -i)$	$(1,\, i,\, -i)$	i

TABLE I. Relevant field content and charge assignment of the model. The notation of SM gauge quantum numbers is given as $(SU(3)_C,\ SU(2)_L)_{U(1)_Y}$.

$$H_1 = \begin{pmatrix} G^+ \\ \frac{v+h+iG}{\sqrt{2}} \end{pmatrix}, \quad H_2 = \begin{pmatrix} H^+ \\ \frac{H+iA}{\sqrt{2}} \end{pmatrix}, \tag{2}$$

where G^+ and G are the SM Nambu-Goldstone bosons, and H^+ and h are a charged Higgs boson and the discovered CP-even Higgs boson, respectively. H and A correspond to additional neutral scalars. The scalar potential of our model is given by

$$\begin{aligned} V = {} & M_1^2 H_1^\dagger H_1 + M_2^2 H_2^\dagger H_2 + \lambda_1 (H_1^\dagger H_1)^2 + \lambda_2 (H_2^\dagger H_2)^2 \\ & + \lambda_3 (H_1^\dagger H_1)(H_2^\dagger H_2) + \lambda_4 (H_1^\dagger H_2)(H_2^\dagger H_1) \\ & + \frac{\lambda_5}{2} (H_1^\dagger H_2)^2 + \text{h.c.}\,. \end{aligned} \tag{3}$$

Since the mass spectrum of the scalars is of crucial importance for the muon $g-2$ as well as the collider phenomenology, we explicitly show the mass relations:

$$\begin{aligned} m_h^2 &= \lambda_1 v^2, \quad m_A^2 = M_{22}^2 + \frac{\lambda_3+\lambda_4-\lambda_5}{2} v^2, \\ m_H^2 &= m_A^2 + \lambda_5 v^2, \quad m_{H^\pm}^2 = m_A^2 - \frac{\lambda_4-\lambda_5}{2} v^2. \end{aligned} \tag{4}$$

For later convenience we define the mass difference of the heavy neutral scalars as

$$\begin{aligned} \Delta_{H-A} &= m_H - m_A \\ &\simeq 50\,\text{GeV} \left(\frac{\lambda_5}{1.5}\right) \left(\frac{1800\,\text{GeV}}{m_H + m_A}\right). \end{aligned} \tag{5}$$

Note that $\lambda_5 \geq 0$ corresponds to $m_H \geq m_A$. The mass difference Δ_{H-A} decreases for heavier scalars, since it is proportional to the $SU(2)_L$ breaking.

#4 In order to obtain realistic neutrino masses and mixings the model needs to be extended. See Ref. [43] for details.

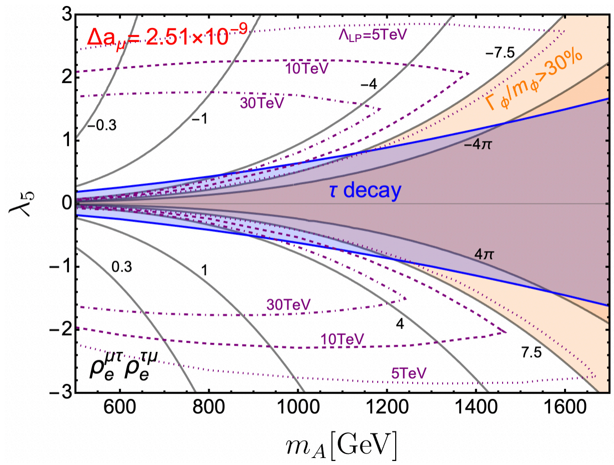

FIG. 2. The black contours show the value of $\rho_e^{\mu\tau}\rho_e^{\tau\mu}$ to explain the central value of α_μ in the m_A vs. λ_5 plane. The blue region is excluded by the lepton flavor universality of τ decays. The orange region corresponds to $\Gamma_\phi/m_\phi \geq 30\%$. The purple contours depict the cutoff scale of the model.

Following the notation in Ref. [21], the Yukawa sector of the model based on the $\mathbb{Z}_4$ charge assignment, in addition to the SM part, is given as

$$-\mathcal{L}_Y = \rho_e^{\mu\tau}\overline{L}_\mu H_2 \tau_R + \rho_e^{\tau\mu}\overline{L}_\tau H_2 \mu_R + \text{h.c.}, \tag{6}$$

where $\rho_e^{\mu\tau}$ and $\rho_e^{\tau\mu}$ are free parameters. In this model, a sizable contribution to Δa_μ is generated via the one-loop diagram mediated by the extra neutral Higgs bosons H and A. The τ mass enhanced contribution is given as [21, 22]

$$\begin{aligned}\Delta a_\mu &\simeq \frac{m_\mu m_\tau \rho_e^{\mu\tau}\rho_e^{\tau\mu}}{16\pi^2}\left(\frac{\ln\frac{m_H^2}{m_\tau^2}-\frac{3}{2}}{m_H^2}-\frac{\ln\frac{m_A^2}{m_\tau^2}-\frac{3}{2}}{m_A^2}\right)\\ &\simeq -2.5\times10^{-9}\left(\frac{\rho_e^{\mu\tau}\rho_e^{\tau\mu}}{1.0}\right)\left(\frac{\lambda_5}{1.0}\right)\left(\frac{700[\text{GeV}]}{m_A}\right)^4,\end{aligned} \tag{7}$$

where Eq. (5) is used to derive the second relation. Fig. 2 shows the value of $\rho_e^{\mu\tau}\rho_e^{\tau\mu}$ required to explain the central value of the discrepancy with black contours.[#5] We are interested in the heaviest possible scenario and thus $|\rho_e^{\mu\tau}| = |\rho_e^{\tau\mu}|$ is set in the following. If we allow for large Yukawa couplings, heavy scalars of $\mathcal{O}(1)$ TeV can explain the muon $g-2$ discrepancy. Furthermore the product of $\rho_e^{\mu\tau}\rho_e^{\tau\mu}\lambda_5$ must be negative to obtain a positive contribution to Δa_μ. In summary we find that the parameters relevant for Δa_μ are $\rho_e^{\mu\tau}\rho_e^{\tau\mu}$, m_A and λ_5. It is noted that the τ mass enhanced $g-2$ contribution picks up the $SU(2)_L$-breaking effect and is proportional to m_A^{-4}.

The charged Higgs mass is set to $m_{H^\pm} = m_A$ ($m_{H^\pm} = m_H$) for $\lambda_5 \geq 0$ ($\lambda_5 \leq 0$) to respect the constraints from electroweak oblique parameters [46] and vacuum stability [47]. The size of the couplings is bounded from above by the requirement that the theory remains perturbative, we hence choose $|\lambda_i| \leq 4\pi$ and $|\rho_e^{\mu\tau}| \leq \sqrt{4\pi}$ [28]. Furthermore, the perturbative unitarity condition for which we require tree-level unitarity of $2\to2$ processes is imposed [48–50]. Even if the couplings satisfy those constraints at the mass scale of the additional scalars, renormalization group (RG) running effects alter them and the theory would become non-perturbative at a high energy scale with $\mathcal{O}(1)$ couplings. To quantify this, we solve the coupled RG equations (RGEs) for β functions of the SM third generation fermion Yukawa couplings, λ_i, $\rho_e^{\mu\tau}$ and $\rho_e^{\tau\mu}$, and then determine the cut-off scale, Λ.[#6] These conditions imply the existence of an upper mass limit for the heavy scalars. In Fig. 2 dash-dotted, dashed and dotted lines in purple depict $\Lambda = 30\,\text{TeV}$, $10\,\text{TeV}$ and $5\,\text{TeV}$. It is observed that if we require the theory to be perturbative up to 30 (5) TeV, the upper limit on the scalar mass is given as

$$m_A \leq 1250\ (1650)\,\text{GeV}. \tag{8}$$

The large λ_5 case is constrained by the $2\to2$ unitarity bound while the small λ_5 region is disfavored by the unitarity constraint on the RGE-evolved Yukawa couplings.

The presence of a charged Higgs with a sizable product of the relevant Yukawa couplings can modify the decay rate of $\tau\to\mu\nu\overline{\nu}$. Following Ref. [27], lepton flavor universality in τ decays puts an upper limit on the interaction:

$$\left|\frac{\rho_e^{\mu\tau}\rho_e^{\tau\mu}}{1.9}\right|\left(\frac{700\text{GeV}}{m_{H^\pm}}\right)^2 \leq 1. \tag{9}$$

The corresponding exclusion is shown in blue in Fig. 2.[#7] Furthermore the one-loop corrections to Z and Higgs boson couplings to $\tau\overline{\tau}$ and $\mu\overline{\mu}$ are known to be less constraining.

[#5] We also include non-m_τ enhanced terms of the neutral scalar loop diagram numerically, however their impact is small in our case. The $H^\pm$-loop contribution does not have an m_τ enhancement and thus its numerical impact is also small.

[#6] See Refs. [28, 51] for the β functions. At the initial scale, we set λ_2, $\lambda_3 \ll 1$ to maximize the cut-off scale. It is noted that there are typos in β functions of Ref. [28].

[#7] The Belle II experiment will improve the sensitivity, however, a quantitative evaluation is not available [52].

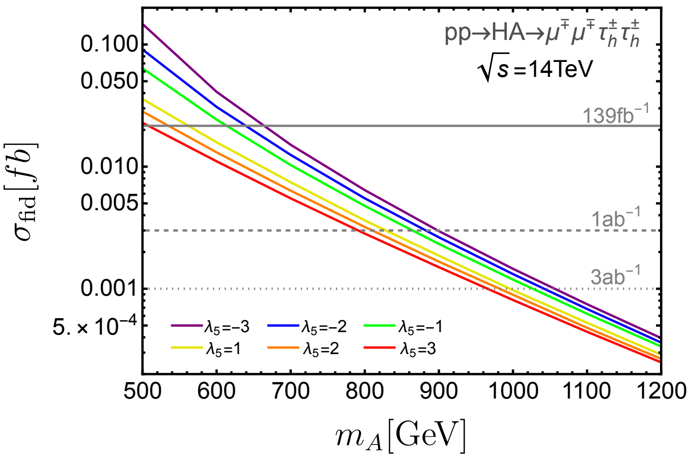

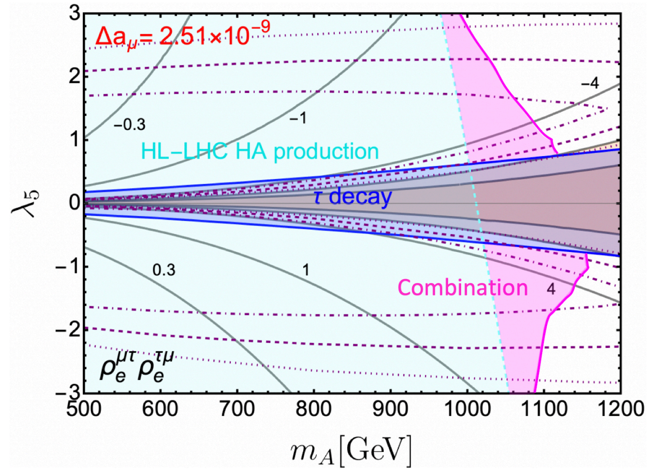

FIG. 3. (Left) Fiducial cross section of $\mu^\pm\mu^\pm\tau_h^\mp\tau_h^\mp$ via electroweak HA production at a 14 TeV pp collider, as a function of m_A in GeV. The horizontal gray lines correspond to the sensitivities with different luminosities. (Right) The collider sensitivities are overlaid on Fig. 2. The cyan region can be tested with 3 ab^{-1} of the electroweak pair production, while the magenta region can additionally be probed by including the single production channel. The blue and orange regions and purple contours are the same as in Fig. 2. $\Delta a_\mu = 2.51 \times 10^{-9}$ is fixed and $|\rho_e^{\mu\tau}| = |\rho_e^{\tau\mu}|$ is assumed in the figure.

Since we are interested in the collider sensitivity utilizing resonant production of the new scalars, the width-to-mass ratio is important. This ratio is approximately given as $\Gamma_\phi/m_\phi \sim |\rho_e^{\mu\tau}|^2 \times 4\%$. We assume that the narrow width approximation is valid up to 30 %. The parameter region which predicts $\Gamma_\phi/m_\phi \geq 30\,\%$ is shown in orange in Fig. 2.

In the early universe the dark matter candidate, S, is in thermal equilibrium with the SM fields through its interaction with the scalar doublet. It is thus possible to explain the relic abundance with the thermal freeze-out mechanism. Thanks to the $\mathbb{Z}_4$ charge assignment, the singlet scalar does not couple to the nucleon at the tree level, evading the stringent constraints from direct detection experiments. However, one-loop Z penguin induced DM-nucleon scattering can constrain the model. The viable mass range for S is broad and the next generation experiments are important to probe the interesting parameter space [43].

We note that charged scalar pair production is probed by the left-handed slepton search [53, 54]. However, it is difficult to constrain O(1) TeV $H^\pm$ with BR($H^\pm \to \mu\nu$) $\simeq 0.5$ even at the HL-LHC.

III. LHC PROBE OF TEV SCALAR SCENARIO

In this section we investigate the LHC sensitivity to our model. As a first step we briefly extend the previous study [30] and evaluate the high luminosity (HL)-LHC reach of the model based on the electroweak pair production of the scalars. Ref. [30] focused on the weakly-coupled scenario with $|\lambda_5|$, $|\rho_e^{\mu\tau}|$, $|\rho_e^{\tau\mu}| \leq 1$, and thus $m_A \leq 700$ GeV was considered. It was argued that the very distinctive $\mu^\pm\mu^\pm\tau^\mp\tau^\mp$ final state via decays of an electroweakly produced pair of neutral scalars is useful to test the model and we showed that 139 fb^{-1} of the data can probe the scenario with $m_A \lesssim 500$ GeV. The electroweak production cross section depends only on the heavy scalar masses.

Throughout our analysis, we use MadGraph5_aMC@NLO [55] with NNPDF3.1luxQED [56] to calculate the signal cross sections. To account for the minimal kinematic cuts, $|p_T^\mu|$, $|p_T^\tau| \geq 20$ GeV, $|\eta_\mu|$, $|\eta_\tau| \leq 2.7$, and $\Delta R \geq 0.1$ are imposed for all pairs of charged leptons. We assume a hadronic τ-tagging efficiency of 70% [57] and the hadronic τ decay branching ratio of about 65% [46]. It is noted that an excellent τ charge reconstruction is reported in Ref. [58]. Our signal of same sign $\mu^\pm\mu^\pm$ and $\tau^\mp\tau^\mp$ pairs of which $\mu^\pm\tau^\mp$ forms a resonance is very distinctive. Specifically, due to the resonance structure, the final-state leptons are very energetic. Therefore we can safely assume the SM background (SMBG) to be negligible.[#8] In this situation Poisson statistics is applicable and the sensitivity at 95% confidence level is given when $\simeq 3$ signal events are predicted, if no events are observed in the data. The additional decay channels $H \to W^\pm H^\mp$ and $A \to HZ$ open in the case of large mass differences. However, such large mass splittings are difficult for $\mathcal{O}(1)$ TeV scalars. We numerically included this dilution effect.

In the presence of a portal interaction between the Higgs doublets and the DM candidate S, invisible scalar decay would suppress BR($\phi \to \mu\tau$) and hence reduce the $\mu^\pm\mu^\pm\tau_h^\mp\tau_h^\mp$ signal number. However, BR($\phi \to \mu\tau$) is proportional to m_ϕ while BR($\phi \to SS$) is proportional to m_ϕ^{-1} because of the dimensionful coupling κv originating

[#8] Background events come from $pp \to ZZ \to 4\tau$. We confirmed that the contribution is smaller than $\mathcal{O}(10^{-5})$ fb and can safely be neglected in the resonant regime.

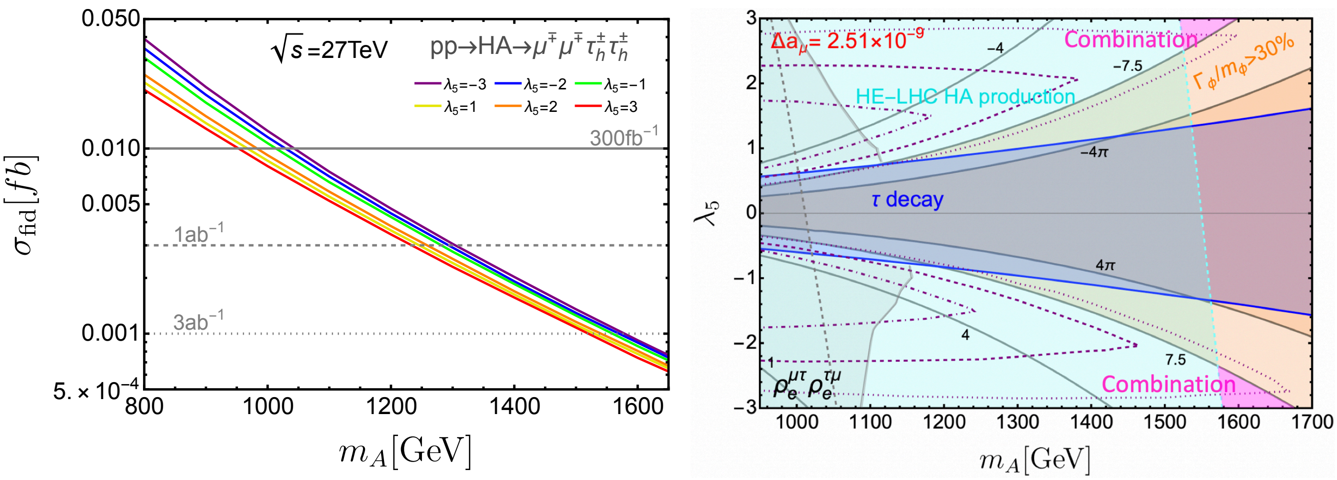

FIG. 4. (Left) Fiducial cross section of $\mu^\pm\mu^\pm\tau_h^\mp\tau_h^\mp$ via electroweak HA production as a function of m_A in GeV. The colored lines show the model prediction at a 27 TeV pp collider. The horizontal gray lines correspond to the sensitivities with different luminosities. (Right) The cyan region shows the sensitivity of the HE-LHC based on HA production. The magenta region can additionally be probed by including single production. The gray region displays the sensitivity of the HL-LHC. See also the caption in Figs. 2 and 3.

from the interaction

$$V \supset \kappa(H_1^\dagger H_2)S^2 + h.c.. \tag{10}$$

As a result $\mathrm{BR}(\phi \to SS)$ is suppressed in the heavy scalar regime and $\mathrm{BR}(\phi \to \mu\tau) \simeq 1$ holds well. Therefore the $\mu^\pm\mu^\pm\tau^\mp\tau^\mp$ mode remains a viable and important probe of the model.

The colored contours in Fig. 3 (left) show the fiducial $\mu^\pm\mu^\pm\tau_h^\mp\tau_h^\mp$ cross sections based on the electroweak HA production with $\sqrt{s} = 14\,\mathrm{TeV}$. The horizontal lines correspond to the sensitivity for integrated luminosities of $139\,\mathrm{fb}^{-1}$, $1\,\mathrm{ab}^{-1}$, and $3\,\mathrm{ab}^{-1}$ and correspond to cross sections of 0.02 fb, 0.003 fb and 0.001 fb, respectively.

Therefore, the HL-LHC data of $1\,\mathrm{ab}^{-1}$ and $3\,\mathrm{ab}^{-1}$ would be sensitive to mass scales of $m_A \simeq 800\,\mathrm{GeV}$ and $m_A \simeq 960\,\mathrm{GeV}$. It is worth mentioning that the pair production channel is powerful since once the neutral scalars are produced they dominantly decay into $\mu\tau$, as long as a sizable τ-mass enhanced contribution to a_μ is postulated. Nevertheless there is a mass gap between the sensitivity and the theoretical upper limit of Eq. (8). The loss of sensitivity for larger m_A mainly comes from two factors: the contributing coupling constant is a weak gauge coupling which is independent of Δa_μ and the production cross section is suppressed by the heaviness of the pair-produced scalars.

One possible way to extend the LHC reach to our model is to include the single heavy scalar production channels corresponding to the middle and right diagrams of Fig. 1. Especially for $\mathcal{O}(1)$ TeV lepto-philic particles the inclusion of the photon initiated process is important [34]. Again, following the procedure in Ref. [24] we assume the SMBG to be negligible. There are two terms in the single scalar production amplitude to generate $\mu^\pm\mu^\pm\tau^\mp\tau^\mp$ events. One is proportional to $(|\rho_e^{\mu\tau}|^2 + |\rho_e^{\tau\mu}|^2)$ which vanishes in the $m_A = m_H$ limit. On the other hand the term proportional to $\rho_e^{\mu\tau}\rho_e^{\tau\mu}$ does not disappear in this limit. Since the m_A^{-4} scaling in Eq. (7) requires a large product of the LFV Yukawa couplings and the first term is suppressed by the mass difference, the second contribution will be important for $\mathcal{O}(1)$ TeV scalars.

In Fig. 3 (right) we overlay the collider sensitivity in the m_A vs. λ_5 plane. The cyan region shows the sensitivity of the pair production channel. The sensitivity is asymmetric in λ_5, since $\lambda_5 \geq 0$ corresponds to $m_H \geq m_A$ and thus the production cross section will be smaller compared to $m_H \leq m_A$. The magenta regions can additionally be covered by including also the single scalar production. We note that there is also a non-resonant signal contribution which comes from t-channel A/H exchange. Since the lepton p_T in this case is generally small and we are interested in the high p_T region where the BG is negligible, this contribution is separated and subtracted to evaluate the sensitivity. We find that the inclusion of the single production process can improve the experimental reach by 130 and 60 GeV for $|\lambda_5| \simeq 1$ and 2, respectively, when the Yukawa couplings are large. This still leaves a gap between the experimental reach and theoretical upper limit.

In order to further boost the sensitivity to the large-mass scenario it is important to increase the center of mass energy from $\sqrt{s} = 14\,\mathrm{TeV}$ to, for instance, 27 TeV [59]. The colored lines in Fig. 4 (left) show the fiducial pair production cross section with $\sqrt{s} = 27\,\mathrm{TeV}$. The horizontal lines correspond to the sensitivity for integrated luminosities of $300\,\mathrm{fb}^{-1}$, $1\,\mathrm{ab}^{-1}$, and $3\,\mathrm{ab}^{-1}$. Thanks to the larger center of mass energy we see that 1250 (1550) GeV can be covered with $1\,(3)\,\mathrm{ab}^{-1}$ of data. It is noted that the same kinematic cut introduced above has been applied for simplicity. The sensitivity is shown in cyan in the right panel.

Again the reach of the $\mu^\pm\mu^\pm\tau^\mp\tau^\mp$ channel can be extended by including the single production process. The magenta regions in Fig. 4 (right) in the right corners can also be probed. Compared to the sensitivity with $\sqrt{s} = 14\,\text{TeV}$ shown in gray on the left, the high energy (HE)-LHC is significantly more sensitive to the heavy scalar scenario. As a result, we observe that all the theoretically viable parameter region in Fig. 4 (right) can be covered.

IV. SUMMARY AND DISCUSSION

The new FNAL experimental data for the muon $g-2$ is consistent with the previously measured value at the Brookhaven experiment, and the significance of the long-standing discrepancy now amounts to $4.2\,\sigma$. In this article we revisited the collider prospects of the $\mathbb{Z}_4$-based 2HDM which can explain the discrepancy using new one-loop contributions involving τ and neutral scalars. A distinctive model prediction is the $\mu^\pm\mu^\pm\tau^\mp\tau^\mp$ signature at the LHC. Since the viable parameter space of the model can not be fully probed at the LHC with the previously proposed electroweak scalar pair production, we investigated the impact of the single scalar production. We have shown that the latter mode helps to extend the reach for the $\mathcal{O}(1)$ TeV scalar solution of the muon $g-2$ discrepancy. For instance, the HL-LHC with $3\,\text{ab}^{-1}$ can test up to $m_A = 1100\,\text{GeV}$. We also examined the search potential at the HE-LHC and showed that increasing the center of the mass energy is crucial to fully probe our scenario. While the model can also explain the DM relic abundance, the reach of the proposed search does not depend on the DM interpretation.

In this article we did not discuss $H^\pm\phi$ production. Due to a combinatorial factor the cross section is four times larger than the one of HA pair production [30]. The final state contains three charged leptons $2\tau+\mu$ or $2\mu+\tau$ and a neutrino at parton level, with their relative rates depending on the ratio of $|\rho_e^{\mu\tau}|^2$ and $|\rho_e^{\tau\mu}|^2$ [29]. Hence $H^\pm\phi$ production is expected to have better sensitivity to $|\rho_e^{\tau\mu}|^2$. Allowing for an imbalance in the couplings, $\rho_e^{\tau\mu} < \rho_e^{\mu\tau}$, while keeping the product $\rho_e^{\tau\mu}\rho_e^{\mu\tau}$ fixed, will thus decrease the LHC sensitivity to the $g-2$ solution in $H^\pm\phi$ production. At the same time the required larger value of $\rho_e^{\mu\tau}$ also lowers the cut-off scale of the theory. Note that the single scalar production cross section, being proportional to $(|\rho_e^{\mu\tau}|^2 + |\rho_e^{\tau\mu}|^2)$, is enhanced in this case. Thus, the signal discussed here is more universal. Combining those various search channels to further enhance the sensitivity would be an interesting future direction.

Motivated by the muon $g-2$ discrepancy, we focused on the 2HDM with $\mu\tau$ LFV couplings. While the $e\mu$- and $e\tau$-philic scenarios lack such motivation, LFV particles can be a viable DM mediator and they predict a similar collider phenomenology. Especially the $e\mu$ case is attractive in this respect, since the particle reconstruction is easier and the fiducial cross section via electroweak pair production is larger by a factor of five since the hadronic τ decay branching ratio and tagging efficiency do no longer reduce the signal rate. This means that the relevant cross sections can be obtained from Fig. 3 and Fig. 4 by lifting the predictions by a factor of five.

ACKNOWLEDGEMENTS

We thank Ulrich Nierste, Shohei Okawa and Yuji Omura for valuable comments and discussion. We enjoy the support from the Deutsche Forschungsgemeinschaft (DFG, German Research Foundation) under grant 396021762-TRR 257. We also appreciate KIT for providing the necessary computational resources. M.B. thanks the Mainz Institute for Theoretical Physics (MITP) of the Cluster of Excellence PRISMA$^+$ (Project ID 39083149) for its hospitality and support during the completion of this project.

---

[1] T. Aoyama *et al.*, Phys. Rept. **887**, 1 (2020), arXiv:2006.04822 [hep-ph].
[2] G. W. Bennett *et al.* (Muon g-2), Phys. Rev. D **73**, 072003 (2006), arXiv:hep-ex/0602035.
[3] B. Abi *et al.* (Muon g-2), Phys. Rev. Lett. **126**, 141801 (2021), arXiv:2104.03281 [hep-ex].
[4] M. Davier, A. Hoecker, B. Malaescu, and Z. Zhang, Eur. Phys. J. C **77**, 827 (2017), arXiv:1706.09436 [hep-ph].
[5] M. Davier, A. Hoecker, B. Malaescu, and Z. Zhang, Eur. Phys. J. C **80**, 241 (2020), [Erratum: Eur.Phys.J.C 80, 410 (2020)], arXiv:1908.00921 [hep-ph].
[6] A. Keshavarzi, D. Nomura, and T. Teubner, Phys. Rev. D **97**, 114025 (2018), arXiv:1802.02995 [hep-ph].
[7] A. Keshavarzi, D. Nomura, and T. Teubner, Phys. Rev. D **101**, 014029 (2020), arXiv:1911.00367 [hep-ph].
[8] M. Cè *et al.*, (2022), arXiv:2206.06582 [hep-lat].
[9] S. Borsanyi *et al.*, Nature **593**, 51 (2021), arXiv:2002.12347 [hep-lat].
[10] C. Alexandrou *et al.*, (2022), arXiv:2206.15084 [hep-lat].
[11] A. Crivellin, M. Hoferichter, C. A. Manzari, and M. Montull, Phys. Rev. Lett. **125**, 091801 (2020), arXiv:2003.04886 [hep-ph].
[12] A. Keshavarzi, W. J. Marciano, M. Passera, and A. Sirlin, Phys. Rev. D **102**, 033002 (2020), arXiv:2006.12666 [hep-ph].
[13] G. Colangelo, M. Hoferichter, and P. Stoffer, Phys. Lett. B **814**, 136073 (2021), arXiv:2010.07943 [hep-ph].
[14] A. Crivellin and M. Hoferichter (2022) arXiv:2207.01912 [hep-ph].
[15] S. Nie and M. Sher, Phys. Rev. D **58**, 097701 (1998), arXiv:hep-ph/9805376.
[16] R. A. Diaz, R. Martinez, and J. A. Rodriguez, Phys. Rev. D **64**, 033004 (2001), arXiv:hep-ph/0010339.

[17] S. Baek, N. G. Deshpande, X. G. He, and P. Ko, Phys. Rev. D **64**, 055006 (2001), arXiv:hep-ph/0104141.
[18] E. O. Iltan and H. Sundu, Acta Phys. Slov. **53**, 17 (2003), arXiv:hep-ph/0103105.
[19] Y.-L. Wu and Y.-F. Zhou, Phys. Rev. D **64**, 115018 (2001), arXiv:hep-ph/0104056.
[20] K. A. Assamagan, A. Deandrea, and P.-A. Delsart, Phys. Rev. D **67**, 035001 (2003), arXiv:hep-ph/0207302.
[21] Y. Omura, E. Senaha, and K. Tobe, JHEP **05**, 028 (2015), arXiv:1502.07824 [hep-ph].
[22] Y. Omura, E. Senaha, and K. Tobe, Phys. Rev. D **94**, 055019 (2016), arXiv:1511.08880 [hep-ph].
[23] J. Heeck, Phys. Lett. B **758**, 101 (2016), arXiv:1602.03810 [hep-ph].
[24] W. Altmannshofer, C.-Y. Chen, P. S. Bhupal Dev, and A. Soni, Phys. Lett. B **762**, 389 (2016), arXiv:1607.06832 [hep-ph].
[25] C.-W. Chiang and K. Tsumura, JHEP **05**, 069 (2018), arXiv:1712.00574 [hep-ph].
[26] P. S. B. Dev, R. N. Mohapatra, and Y. Zhang, Phys. Rev. Lett. **120**, 221804 (2018), arXiv:1711.08430 [hep-ph].
[27] S. Iguro and Y. Omura, JHEP **05**, 173 (2018), arXiv:1802.01732 [hep-ph].
[28] Y. Abe, T. Toma, and K. Tsumura, JHEP **06**, 142 (2019), arXiv:1904.10908 [hep-ph].
[29] L. Wang and Y. Zhang, Phys. Rev. D **100**, 095005 (2019), arXiv:1908.03755 [hep-ph].
[30] S. Iguro, Y. Omura, and M. Takeuchi, JHEP **11**, 130 (2019), arXiv:1907.09845 [hep-ph].
[31] A. Crivellin, D. Müller, and C. Wiegand, JHEP **06**, 119 (2019), arXiv:1903.10440 [hep-ph].
[32] M. Bauer, M. Neubert, S. Renner, M. Schnubel, and A. Thamm, Phys. Rev. Lett. **124**, 211803 (2020), arXiv:1908.00008 [hep-ph].
[33] C. Cornella, P. Paradisi, and O. Sumensari, JHEP **01**, 158 (2020), arXiv:1911.06279 [hep-ph].
[34] S. Iguro, K. A. Mohan, and C. P. Yuan, Phys. Rev. D **101**, 075011 (2020), arXiv:2001.09079 [hep-ph].
[35] S. Iguro, Y. Omura, and M. Takeuchi, JHEP **09**, 144 (2020), arXiv:2002.12728 [hep-ph].
[36] S. Jana, V. P. K., and S. Saad, Phys. Rev. D **101**, 115037 (2020), arXiv:2003.03386 [hep-ph].
[37] H.-X. Wang, L. Wang, and Y. Zhang, Eur. Phys. J. C **81**, 1007 (2021), arXiv:2104.03242 [hep-ph].
[38] A. J. Buras, A. Crivellin, F. Kirk, C. A. Manzari, and M. Montull, JHEP **06**, 068 (2021), arXiv:2104.07680 [hep-ph].
[39] N. Ghosh and J. Lahiri, Eur. Phys. J. C **81**, 1074 (2021), arXiv:2103.10632 [hep-ph].
[40] W.-S. Hou, R. Jain, C. Kao, G. Kumar, and T. Modak, Phys. Rev. D **104**, 075036 (2021), arXiv:2105.11315 [hep-ph].
[41] X.-F. Han, F. Wang, L. Wang, J. M. Yang, and Y. Zhang, Chin. Phys. C **46**, 103105 (2022), arXiv:2204.06505 [hep-ph].
[42] J. Kriewald, J. Orloff, E. Pinsard, and A. M. Teixeira, Eur. Phys. J. C **82**, 844 (2022), arXiv:2204.13134 [hep-ph].
[43] K. Asai, C. Miyao, S. Okawa, and K. Tsumura, Phys. Rev. D **106**, 035017 (2022), arXiv:2205.08998 [hep-ph].
[44] H. Georgi and D. V. Nanopoulos, Phys. Lett. B **82**, 95 (1979).
[45] J. F. Donoghue and L. F. Li, Phys. Rev. D **19**, 945 (1979).
[46] P. A. Zyla *et al.* (Particle Data Group), PTEP **2020**, 083C01 (2020).
[47] M. Sher, Phys. Rept. **179**, 273 (1989).
[48] B. W. Lee, C. Quigg, and H. B. Thacker, Phys. Rev. D **16**, 1519 (1977).
[49] S. Kanemura, T. Kubota, and E. Takasugi, Phys. Lett. B **313**, 155 (1993), arXiv:hep-ph/9303263.
[50] A. Arhrib, in *Workshop on Noncommutative Geometry, Superstrings and Particle Physics* (2000) arXiv:hep-ph/0012353.
[51] S. Iguro, S. Okawa, and Y. Omura, (2022), arXiv:2208.05487 [hep-ph].
[52] W. Altmannshofer *et al.* (Belle-II), PTEP **2019**, 123C01 (2019), [Erratum: PTEP 2020, 029201 (2020)], arXiv:1808.10567 [hep-ex].
[53] G. Aad *et al.* (ATLAS), Phys. Rev. D **101**, 052005 (2020), arXiv:1911.12606 [hep-ex].
[54] G. Aad *et al.* (ATLAS), Eur. Phys. J. C **80**, 123 (2020), arXiv:1908.08215 [hep-ex].
[55] J. Alwall, R. Frederix, S. Frixione, V. Hirschi, F. Maltoni, O. Mattelaer, H. S. Shao, T. Stelzer, P. Torrielli, and M. Zaro, JHEP **07**, 079 (2014), arXiv:1405.0301 [hep-ph].
[56] V. Bertone, S. Carrazza, N. P. Hartland, and J. Rojo (NNPDF), SciPost Phys. **5**, 008 (2018), arXiv:1712.07053 [hep-ph].
[57] ATLAS(ATL-PHYS-PUB-2019-033), .
[58] ATLAS(ATL-PHYS-PUB-2015-025), .
[59] A. Abada *et al.* (FCC), Eur. Phys. J. ST **228**, 1109 (2019).